Science of the Total Environment 838 (2022) 155988

Contents lists available at ScienceDirect

Science of the Total Environment

journal homepage: www.elsevier.com/locate/scitotenv

Evaluation of carbon sink in the Taklimakan Desert based on correction of abnormal negative CO_2 flux of IRGASON

Fan Yang [a,b], Jianping Huang [c,*], Xinqian Zheng [d], Wen Huo [a], Chenglong Zhou [a,b], Yu Wang [a], Dongliang Han [c], Jiacheng Gao [a], Ali Mamtimin [a], Xinghua Yang [a], Yingwei Sun [e]

[a] Institute of Desert Meteorology, China Meteorological Administration/National Observation and Research Station of Desert Meteorology, Taklimakan Desert of Xinjiang/Taklimakan Desert Meteorology Field Experiment Station of China Meteorological Administration/Xinjiang Key Laboratory of Desert Meteorology and Sandstorm/Key Laboratory of Tree-ring Physical and Chemical Research, China Meteorological Administration, Urumqi 830002, China
[b] College of Atmospheric Sciences, Lanzhou University, Lanzhou 730000, China
[c] Collaborative Innovation Center for Western Ecological Safety, Lanzhou University, Lanzhou 730000, China
[d] Xinjiang Agro-Meteorological Observatory, Urumqi 830002, China
[e] Xinjiang Information Engineering School, Urumqi 830002, China

HIGHLIGHTS

- IRGASON often has abnormal CO_2 uptake signals in desert, which need to be corrected.
- The change of desert soil air volume caused by heat transfer dominates CO_2 exchange.
- The shifting sand of the Taklimakan Desert act as a stable carbon sink.

GRAPHICAL ABSTRACT

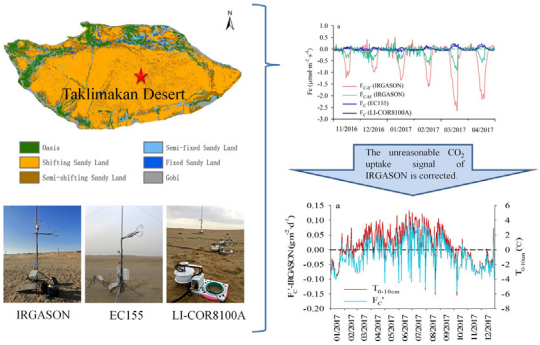

ARTICLE INFO

Editor: Pingqing Fu

Keywords:
Taklimakan Desert
CO_2 flux
Open- and closed-path eddy correlation
Expansion/contraction of soil air
Carbon sequestration capacity

ABSTRACT

Studies showing that deserts can sequester CO_2 through non-photosynthetic processes have contributed to locating missing carbon sinks. However, the contradiction between the desert CO_2 flux obtained by different observation methods leads to uncertainty in evaluating desert carbon sequestration. This has caused scepticism regarding desert carbon sequestration after years of research. Through a comparative experiment in the non-vegetated shifting sand of the Taklimakan Desert (TD), it was found that if the abnormal negative CO_2 flux observed by IRGASON during the day was not corrected, the carbon sequestration of the TD would be overestimated. The CO_2 flux observed by EC155 is highly consistent with that of LI-COR8100A and can reflect the real CO_2 exchange in the desert. The CO_2 flux observed by EC155 was used to correct the results of IRGASON. Results show that the expansion/contraction of soil air containing CO_2 caused by the change in the daily average soil temperature difference ($T_{0–10cm}$) drives CO_2 exchange in shifting sand. This results in diurnal variation of CO_2 release caused by shifting sand during the day and CO_2 absorption at night, and a unimodal distribution of CO_2 exchange caused by shifting sand throughout the year. From April to September ($T_{0–10cm} > 2$ °C), the shifting sand releases CO_2 as a carbon source. In the other months ($T_{0–10cm} < 2$ °C), the shifting sand absorbs CO_2 as a carbon sink. The stronger absorption shows that the shifting sand in the TD provides carbon sequestration, with a CO_2 uptake rate of ~148.85×10^4 tons a^{-1}. This suggests that deserts play an active role in locating the missing carbon sinks and mitigating climate change, and that the status of deserts in the global carbon cycle cannot be ignored.

* Corresponding author at: College of Atmospheric Sciences, Lanzhou University, Lanzhou 730000, China.
E-mail address: hjp@lzu.edu.cn (J. Huang).

http://dx.doi.org/10.1016/j.scitotenv.2022.155988
Received 30 March 2022; Received in revised form 11 May 2022; Accepted 11 May 2022
Available online 16 May 2022

1. Introduction

The eddy covariance technique can obtain turbulent flux values by calculating the covariance between the horizontal wind speed component or the material concentration and the vertical wind speed based on high-frequency three-dimensional wind speed, temperature, CO_2 and water vapour concentration (Baldocchi, 2008). It can accurately evaluate an ecosystem's carbon source-sink intensity and water and energy balances through long-term positioning, continuous, and networking observations with minimal environmental interference. In addition, it can work in coordination with the ecosystem processes and changes in environmental factors to carry out comprehensive and detailed observational experiments (Baldocchi, 2014). This technique is gradually considered the most reliable method to deeply understand the characteristics of material and energy exchange between ecosystems and the atmosphere and their interactions. There are more than 5000 eddy covariance observation stations in the International Flux Observation and Research Network (FLUXNET) (Yu and Sun, 2017).

Desert ecosystems, as typical widely distributed extreme environments, have received much interest from the scientific community in recent years because they can store large amounts of CO_2, reduce the gap in the missing carbon sink, and play a positive role in mitigating climate warming (Stone, 2008; Wohlfahrt et al., 2008; Wang et al., 2016; Yang et al., 2020a, 2020b; Gao et al., 2021). Observations of open-path eddy covariance in desert ecosystems have found that the carbon sequestration rates in the Mojave, Gurbantunggut, Mu Us, and Taklimakan deserts are 100 g m^{-2} a^{-1}, 49 g m^{-2} a^{-1}, 77 g m^{-2} a^{-1} and 146 g m^{-2} a^{-1}, respectively (Schlesinger, 2017; Jasoni et al., 2005; Wohlfahrt et al., 2008; Liu et al., 2012; Jia et al., 2014). However, few problems still exist with regard to desert carbon sequestration: lack of precise information about the storage locations of CO_2 taken up by deserts, no reasonable explanation for a higher reported amount of desert carbon sequestration than that of the net primary productivity of desert ecosystems (Schlesinger, 2017); and the phase and magnitude contradiction between the CO_2 flux obtained by the open-path eddy covariance method and other observation methods (e.g. soil respiration and closed-path eddy covariance). These problems make the application of open-path eddy covariance in desert ecosystems challenging, and the study of desert carbon sinks remains questionable even after many years of research. Therefore, solving the contradiction between open-path eddy covariance findings and those of other observation methods and accurately evaluating the effect of applying open-path eddy covariance in desert ecosystems is the basis of desert carbon sink research.

The traditional open-path eddy covariance system comprises an open-path infrared gas analyser (IRGA) and a separate three-dimensional sonic anemometer. Because of the heterotopic space between the two sensors and the shape design of the IRGA, observation accuracy is always limited by spatial separation, temporal asynchronicity, and self-heating effects (Bogoev, 2014; Moore, 1986; Burba et al., 2008). With the integration of the IRGA and sonic anemometers, the infrared temperature is replaced by sonic temperature, reducing sensor power consumption and the need for the application of a series of correction algorithms (e.g. model IRGASON, LI-COR Inc.), as well as partially solving the measurement accuracy problems caused by the interference effects of spatial separation, time synchronisation, and self-heating (Wang et al., 2016). To measure the closed-path eddy covariance, gas is pumped into the cavity of the built-in IRGA. Although this measurement method faces problems caused by high-frequency signal loss and the time lag between measuring the gas concentration and detection by the sonic anemometer, it is considered to have high measurement accuracy due to less interference from the external environment (Yu and Sun, 2017). However, there are still differences in comparative experiments that measure CO_2 flux using open- and closed-path eddy covariance methods (Song et al., 2005; Haslwanter et al., 2009; Helbig et al., 2016;). According to the analyses, this systematic bias may be caused by spectroscopic effects (e.g. absorption line broadening) on the IRGAs used in the open-path eddy covariance method (Detto et al., 2011). The bias becomes more obvious when the "real" CO_2 flux of the ecosystem is low, which manifests as a physiologically unreasonable CO_2 uptake signal (Ham and Heilman, 2003; Ono et al., 2008; Helbig et al., 2016). Desert ecosystems are susceptible to this phenomenon and show unrealistic peak CO_2 absorption signals at noon every day (Wang et al., 2016). This leads to an overestimation of the capacity of desert carbon sinks. Many scientists suggest that this bias is due to the use of low-frequency temperature measurements to determine the high-frequency CO_2 concentration of the IRGA (Wang et al., 2017; Helbig et al., 2016; Russell et al., 2019). Campbell Scientific released a correction method for this bias in May 2017. This method can correct temperature-induced spectroscopic effects and improve the observation effect of CO_2 flux in the northern latitude ecosystem dominated by sensible heat (Campbell Scientific, 2017).

The Taklimakan Desert (TD) is the world's second-largest shifting desert and has the characteristics of being far from the sea, with a dry climate, sparse vegetation, complex dune types, strong dune mobility, large areas of shifting sand, a thick shifting sand layer, and small sand particle size (Yang et al., 2021). It is representative of the world's deserts. Recent studies show that shifting sand in the TD absorbs atmospheric CO_2 at a rate of 1.6 million tons per year (Yang et al., 2020a, 2020b). However, the contradiction between the CO_2 flux of the desert obtained using different observation methods leads to uncertainty in evaluating the carbon sequestration capacity of the TD. This study compared the synchronous observation difference between the open- and closed-path eddy covariance in the non-vegetated shifting sandy land of the TD. In addition, the CO_2 flux obtained by open- and closed-path eddy covariance was evaluated using synchronous soil respiration observations obtained by LI-8100A (LI-COR, Lincoln, NE, USA). On this basis, the influence of environmental factors on the bias of CO_2 flux data obtained by open- and closed-path eddy covariance methods was analysed, and the corresponding correction relationship was established. Using this regression relationship, the CO_2 flux data observed by IRGASON were corrected to analyse the changes in the CO_2 exchange of shifting sand and estimate the carbon sequestration capacity of shifting sand in the TD. This will help further understand the status of deserts in the global carbon cycle and lay a foundation for locating missing carbon sinks.

2. Materials and methods

2.1. Site description

The total area of the TD is 33.7 × 10^4 km^2, of which approximately 70% is covered by continuously shifting sand (Wang et al., 2005; Yang et al., 2021). The field evaluation experiment was conducted at the National Observation and Research Station of Desert Meteorology, Taklimakan Desert of Xinjiang (Fig. 1), located in the hinterland of the TD (38° 58′ N, 83° 39′ E, 1099 m above sea level). This station is considered the most representative station for the study of TD. The region has a continental, warm temperate, arid desert climate. Precipitation is mainly concentrated from May to August and rarely occurs in other months, with an average annual rainfall of only 25.9 mm. The annual potential evaporation is 3812.3 mm, nearly 150 times the annual average precipitation. The mean annual temperature is 12.1 °C, with maximum temperatures of 46.0 °C and minimum temperatures of −32.6 °C. Extremely harsh environmental conditions lead to almost no distribution of animals and plants in this area, and the surface is covered with a constantly shifting sand layer. This provides an excellent environment for dust storm development. According to statistics, the region experiences prevailing easterly winds throughout the year, with an average annual wind speed of 2.3 m·s^{-1} and more than 157 days with floating dust and blowing sand and an annual mean of 16 days with sandstorms (Yang et al., 2021). Soil respiration was significantly lower and was often negative at night in shifting sand. The daily mean rate of soil respiration of shifting sand was 28.7 × 10^{-3} μmol·m^{-2}·s^{-1}, and the daily variation ranged from −0.026 to 0.101 μmol·m^{-2}·s^{-1} (Yang et al., 2017; Yang et al., 2020a, 2020b).

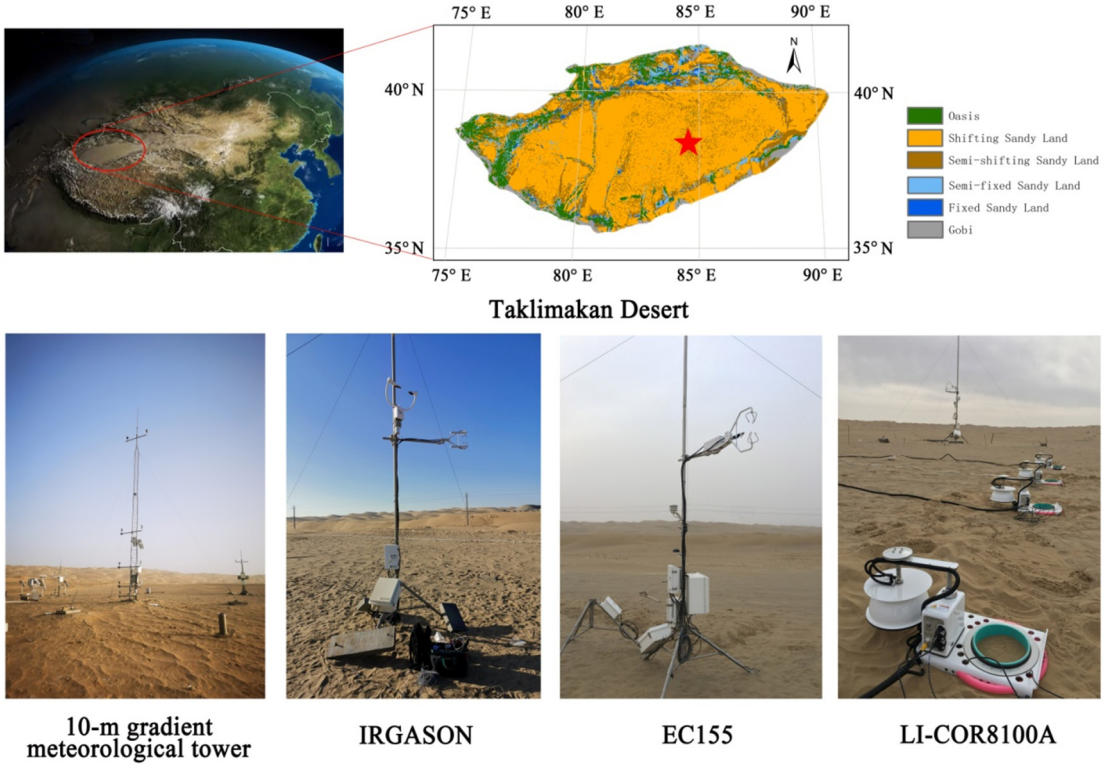

Fig. 1. Upper: Distribution of land cover types in the Taklimakan Desert (TD) and location of the National Observation and Research Station of Desert Meteorology, Taklimakan Desert of Xinjiang (red star). Below: The layout of instruments used in the field evaluation experiment.

2.2. Experimental design

Since 2006, the meteorological environment of the TD has been consistently observed using a 10-m gradient meteorological observation tower in the non-vegetated shifting sand region 1 km west of the station. Fig. 1 and Table 1 provide a detailed description of the instruments used in the experiment. One calibrated open-path and one closed-path eddy covariance system were installed in November 2016. The distance between them was 200 m, and they were installed 3 m above the ground. The 2.5 m short intake tubes and a flow rate of 8 L min^{-1} were used to minimise the temporal asynchronicity and spectral attenuation when installing the closed-path eddy covariance (Novick et al., 2013; Helbig et al., 2016). The comparative observation period was from November 2016 to April 2017. The IRGASON's infrared analyser was cleaned every three days to ensure signal strength. In addition, IRGASON's data collection program was upgraded to the latest EC100 OS version 8.02 (Campbell Scientific Inc.) in January 2021. Using the EC100 OS 8.02, two 30 min CO_2 fluxes were obtained by IRGASON: one is the low-frequency CO_2 flux calculated using the CO_2 density that had not been correct for the spectroscopic effects ($F_{C\text{-}lf}$), and the other is the high-frequency CO_2 flux calculated using the corrected CO_2 density ($F_{C\text{-}hf}$). Based on the relationship between high- and low-frequency CO_2 flux differences and sensible heat, we corrected IRGASON's

Table 1
Summary of the instruments used in this experiment.

Observation system	Observation variables	Sensors	Height/depth (m)	Operation period
10-m gradient meteorological tower	Gradient of the wind speed and direction	WindObserver II-65 (Gill Instruments Ltd.)	0.5, 1.0, 2.0, 4.0, 10.0	Jun 2006 - Now
	Gradient of the T_a and RH	HMP155A (Vaisala Inc.)		
	Press	PTB330 (Vaisala Inc.)	1.5	
	DR, UR, DLR, ULR, Rn	CNR4 (Kipp and Zonen B. V.)	1.5	
	Gradient of the soil temperature	109 (Campbell Scientific Inc.)	0.0, −0.05, −0.1, −0.2, −0.4	
	Gradient of the soil moisture	93640Hydra (Stevens Inc.)	−0.05, −0.1, −0.2, −0.4	
IRGASON	Three-dimensional wind speed and direction, T_a, CO_2/H_2O concentration, H, LE, u_*, $F_{C\text{-}lf}$, $F_{C\text{-}hf}$	IRGASON (Campbell Scientific Inc.)	3.0	Nov 2016 - Dec 2017 Jan 2021 - Dec 2021
EC155	Three-dimensional wind speed and direction, T_a, CO_2/H_2O concentration, H, LE, F_C, u_*	EC155 (Campbell Scientific Inc.)	3.0	Nov 2016 - Apr 2017
LI-COR8100A	Soil CO_2 flux	LI-COR8100A (LI-COR Inc.)	0.0	Nov 2016 - Apr 2017

Where T_a, RH, Press, u_*, F_C, $F_{C\text{-}lf}$, $F_{C\text{-}hf}$, DR, UR, DLR, ULR, and Rn are air temperature, relative humidity, atmospheric pressure, friction velocity, CO_2 flux, low-frequency CO_2 flux, high-frequency CO_2 flux, total solar radiation, ground-reflected radiation, atmospheric long-wave radiation, ground long-wave radiation, and net radiation, respectively.

low-frequency CO_2 flux from November 2016 to April 2017 to eliminate the spectroscopic effects. For the detailed calculation method for this problem, please refer to the announcement issued by Campbell Scientific on 23 May 2017 (Campbell Scientific, 2017).

A LI-COR8100A equipped with a LI-COR8100–104 long-term monitoring chamber was installed under a 10 m meteorological tower to obtain hourly CO_2 flux data in the study area. Because of the weak CO_2 flux in the desert, the LI-COR8100A was calibrated before installation, and the measurement time of the monitoring chamber was set to 150 s. During the observations, the air in the chamber was pumped into the analyser in a constant environment. The soil CO_2 flux was calculated by measuring the real-time change in CO_2 concentration. This method has very high accuracy ($\pm$ 0.02 μmol $m^{-2} s^{-1}$) (Yang et al., 2020a). Although there are differences in the observation principles and representative ranges between the soil respiration instruments and the eddy covariance method, we consider that the CO_2 flux observation by both methods should be equal because the study area is a non-vegetated flat shifting sandy land. Therefore, we considered the data from the soil respiration instrument as a reference to evaluate the effects of open- and closed-path eddy covariance analyses. In addition, due to frequent dust weather in spring and summer in the study area, the LI-COR8100A and EC155 instruments were shut down after April 2017 to avoid pumping many dust particles into the analyser. The corresponding data were missing during the observational period. This is one of the main reasons why instruments with air-pump components cannot operate for a long time in desert areas.

2.3. Data processing

All the eddy covariance data were measured at a frequency of 10 Hz. We calculated the fluxes of sensible heat, latent heat and CO_2 every 30 min using the EasyFlux PC of the Campbell Scientific software. Data processing included the detection and removal of peaks (Vickers and Mahrt, 1997), trend correction (Rannik and Vesala, 1999), two-dimensional coordinate rotation (Wilczak et al., 2001), frequency response correction (Moore, 1986), sonic temperature correction (Schotanus et al., 1983), and Webb–Pearman–Leuning (WPL) density correction (Webb et al., 1980). In addition, flux measurements were classified as high (0), moderate (1), or low-quality (2) data. In this analysis, only the flux measurements marked with quality levels 0 or 1 were used, and the flux data marked with 2 and those taken during precipitation were eliminated. A negative flux indicates transport to the ground, and a positive flux indicates transport to the atmosphere.

2.4. Statistical analyses

We used SigmaPlot 14.0 to conduct the regression analysis on the wind speed (U), friction velocity (u_*), air temperature (T_a), sensible heat flux (H), latent heat flux (LE) and CO_2 flux (F_C) obtained by IRGASON and EC155. In addition, the correlations between the difference in CO_2 flux obtained by IRGASON and EC155 and environmental factors (including air temperature (T_a), air humidity (RH), atmospheric pressure (Press), sensible heat flux (H), total solar radiation (DR), ground reflected radiation (UR), atmospheric long-wave radiation (DLR), ground long-wave radiation (ULR), and net radiation (Rn)) were analysed. Regression analysis was carried out for the difference in CO_2 flux obtained by IRGASON and EC155, and the environmental factors showed high correlations. Using this regression relationship, the abnormal negative CO_2 flux data observed by IRGASON during the day were corrected to obtain the variation in the CO_2 flux of shifting sand in the TD hinterland in 2017. Finally, combined with the surface coverage type of the TD, the carbon sink capacity of shifting sands in the TD was estimated.

3. Results and discussion

3.1. Meteorological conditions

The variation in the half-hour average value of the micrometeorological parameters in the study area during the observation period is shown in Fig. 2. Dust storms and sand-blowing weather often occurred in spring in the study area, resulting in a gradual increase in wind speed after March 2017. The average wind speed in the study area was 1.27 $m \cdot s^{-1}$. The maximum wind speed was 9.34 $m \cdot s^{-1}$, which occurred during a dust storm on 20 March 2017. During the observation period, the average air temperature was 0.2 °C. The air temperature continued to decrease after November 2016, and then gradually increased after reaching the lowest value of −24.7 °C on 15 January 2017. It reached the highest value of 24.9 °C on 3 April 2017. The change in soil temperature was consistent with that in air temperature. With the deepening of the soil layer, the soil temperature showed an obvious gradient order, and the diurnal fluctuation gradually weakened. Because of the extreme drought in the Taklimakan Desert, vapour pressure was maintained at a low level during the observation period. It ranged from 0.48 hPa to 7.10 hPa, with an average value of 2.38 hPa. The soil moisture at a depth of 10 cm was maintained at approximately 0.02%. However, there was a small amount of snow in the study area during the winter. Snowfall on 21 February 2017 resulted in a 1 cm snow cover on the ground. The melting of snow strongly impacted vapour pressure and soil moisture, which increased the vapour pressure and soil moisture at 10 cm to 7.10 hPa and 0.1%, respectively.

3.2. Consistency comparison of observation results of IRGASON and EC155

The consistency of U, u_* and T_a observed by IRGASON and EC155 sonic anemometers was analysed. As shown in Fig. 3, the U and T_a values obtained using the two instruments were in good agreement ($R^2 = 0.995$, $P < 0.01$). The U obtained by EC155 was only 2% higher than that obtained by IRGASON, and the T_a obtained by EC155 was only 1% lower than that

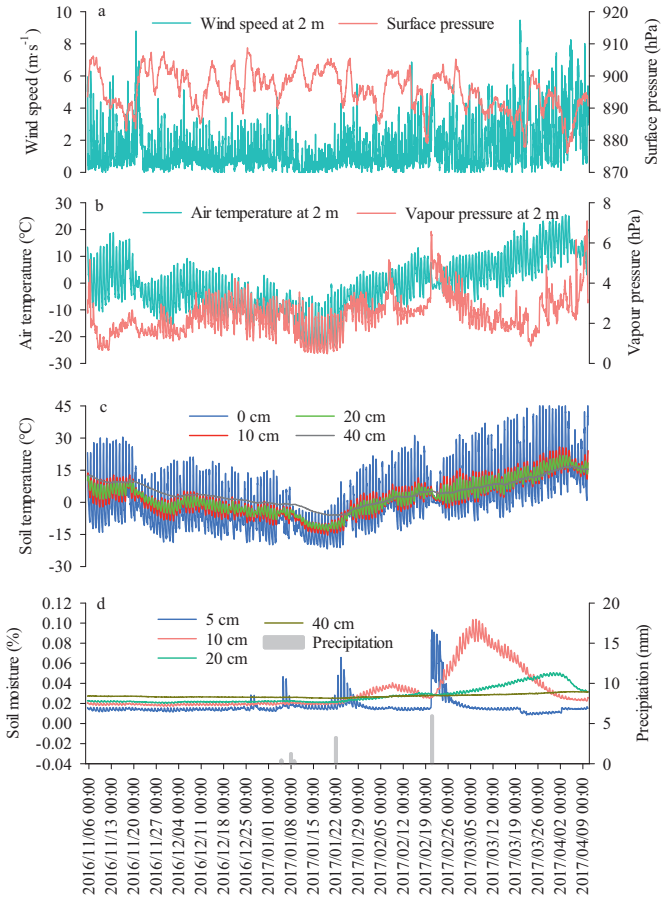

Fig. 2. Time series of micrometeorological parameters per half hour during the observation period from November 2016 to April 2017. a, Wind speed at 2 m and Surface pressure. b, Air temperature at 2 m and Vapour pressure at 2 m. c, Gradient of the soil temperature. d, Gradient of the soil moisture and precipitation.

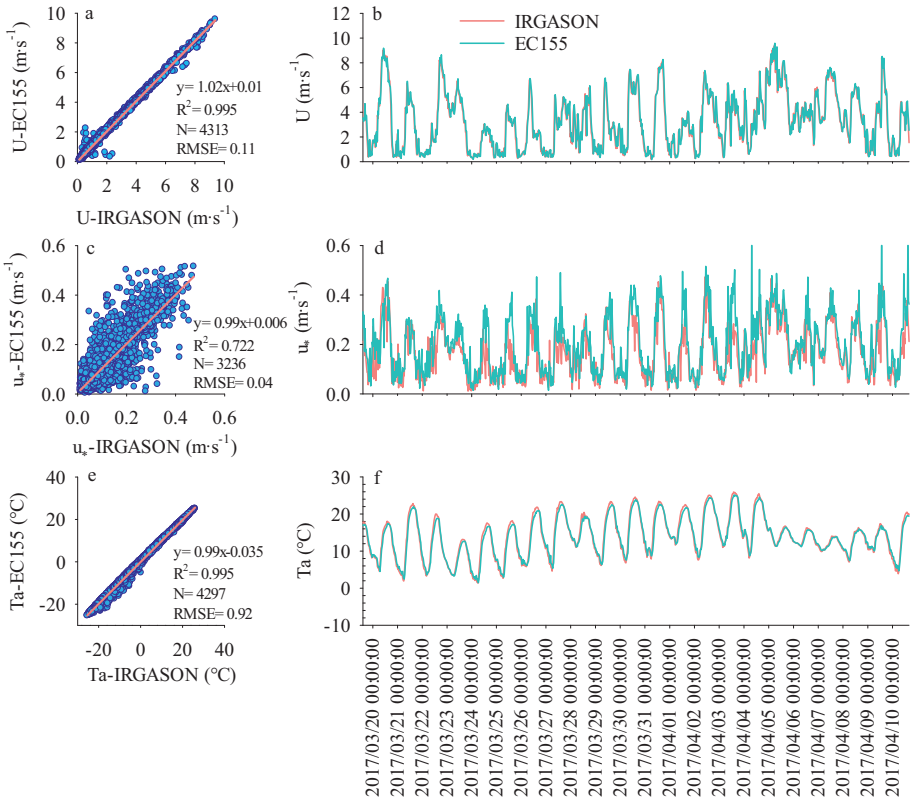

Fig. 3. Differences in half-hourly wind speed (U), friction velocity (u_*) and air temperature (T_a) observed by the sonic anemometer of IRGASON and EC155 were compared. a, c, and e show the data in all observation periods. b, d, and f show the data from March 20 to April 10, 2017.

obtained by IRGASON. For u_*, the two observed values also showed good consistency ($R^2 = 0.722$, $P < 0.01$), but the agreement was weaker than that for U and T_a. This may be closely related to airflow disturbance caused by the scattered and fast-moving small sand dunes around EC155. The u_* obtained by EC155 is 1% lower than that of IRGASON. The difference is within the range of variation (3–15%) of the comparison results of other anemometers (El-Madany et al., 2013; Wang et al., 2016).

The extremely arid environment in the study area leads to a small LE, and a large H. H is the main way of surface energy consumption. Fig. 4 shows that the H values obtained by the two instruments were in good agreement ($R^2 = 0.837$, $P < 0.01$). The ultra-low water vapour content in the hinterland of the desert and the difference in observation methods between the two instruments may amplify the systematic error of the observation instruments, resulting in low consistency of LE between the two instruments. The LE measurement between the two instruments often showed the greatest difference at high values. However, they all show a consistent pattern of changes of similar magnitude. Surprisingly, the changes in the rhythm of the F_C between the two instruments were opposite, and the magnitudes were very different. The IRGASON observation results showed that shifting sand can strongly sequester CO_2 during the day. This strong abnormal negative F_C observation has occurred many times in observational experiments on low-productivity ecosystems (Ono et al., 2008; Wang et al., 2016; Helbig et al., 2016; Liu et al., 2012; Jia et al., 2014). Suppose the unreasonable CO_2 uptake signal of IRGASON in the desert is not corrected. In that case, it will lead to an overestimation of the carbon sequestration capacity of the desert and increase doubts about desert carbon sequestration. In contrast, the F_C obtained using EC155 appeared to be more reasonable. This problem will be further analysed in the following section.

3.3. Evaluation of unreasonable negative CO_2 flux observed by IRGASON

According to the latest data collection program released by Campbell Scientific, the high- and low-frequency values of CO_2 flux ($F_{C\text{-}lf}$ and $F_{C\text{-}hf}$) in 2021 were obtained by IRGASON. The comparison between the high- and low-frequency values indicated significant discrepancies, especially in the range of negative values (Fig. 5a). This result is different from the highly consistent results of Helbig et al. (2016) in eight northern ecosystems and Russell et al. (2019) in North American farmlands. According to the correction method released by Campbell Scientific, the low-frequency CO_2 flux observed from November 2016 to December 2017 was corrected by using the relationship in Fig. 5b, and the high-frequency CO_2 flux in this period was obtained (Campbell Scientific, 2017).

To verify the authenticity of the CO_2 flux data observed by IRGASON and EC155, soil CO_2 flux synchronously observed by LI-COR8100A was used as a reference. Fig. 6a shows the monthly average daily variation in the CO_2 flux obtained by the three instruments during the synchronous observation period. The CO_2 flux observed by EC155 was in good agreement with LI-COR8100A in terms of magnitude and rhythm of change. They all show that shifting sand can release CO_2 during the day and reach a peak at noon; at night, shifting sand can absorb atmospheric CO_2 and show carbon sequestration. This phenomenon has also been observed in experimental observations of the TD, Mu Us desert, and Gurbantunggut desert (Ma et al., 2013, 2014; Yang et al., 2017; Yang et al., 2020a; Fa et al., 2014, 2016; Gao et al., 2021). In addition, Yang et al. (2020a) found that both the expansion/contraction of soil air containing CO_2 caused by heat fluctuations in shifting sand and the salt/alkali chemistry control the CO_2 release/absorption processes of soil. This explains why shifting sand in deserts releases CO_2 during the day and absorbs CO_2 at night. This also increases the confidence that the observation results from EC155 reflect the real desert CO_2 flux and provide a reference for selecting instruments for CO_2 flux observations in deserts. For IRGASON, both high- and low-frequency values showed unreasonably negative values during the day. Compared with the low-frequency value, the daytime negative CO_2 flux shown by the high-frequency value was weakened, but it was still very different from the observation results of EC155 and LI-COR8100A. This indicates that the application of high-frequency CO_2 flux can accurately

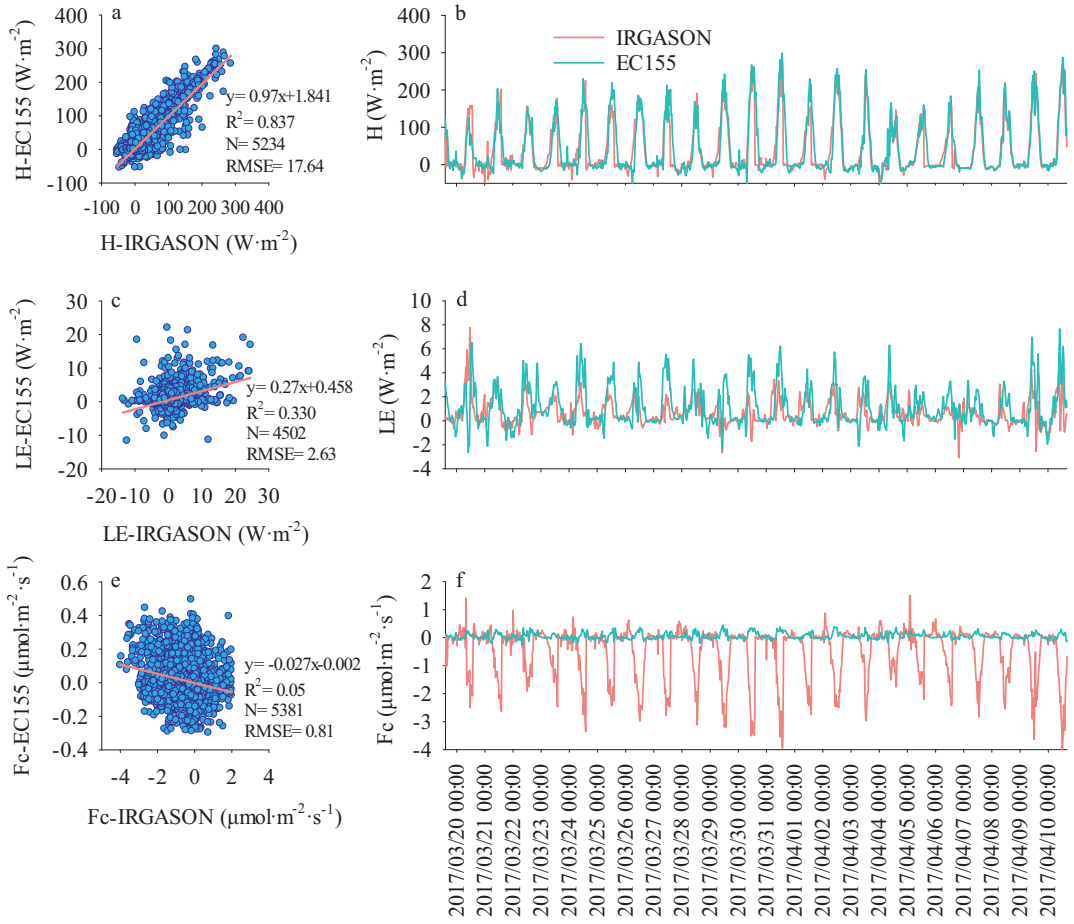

Fig. 4. Differences in half-hourly sensible heat flux (H), latent heat flux (LE) and CO_2 flux (F_C) observed by IRGASON and EC155 were compared. a, c, and e show the data in all observation periods. b, d, and f show the data from March 20 to April 10, 2017.

correct the temperature-induced spectroscopic effects in the forest, grassland, farmland, swamp, and other ecosystems to eliminate the unreasonable negative CO_2 flux during the daytime. However, the correction effect of this method was poor in the desert ecosystems (Fig. 6a and b).

3.4. Further correction of unreasonable negative CO_2 flux during the day observed by IRGASON

Considering the difference in the observation methods of open- and closed-path eddy covariance and the good application effect of high-frequency CO_2 flux in forests and other ecosystems, we suggest that the incomplete correction of self-heating and spectroscopic effects caused by an extremely arid environment, high-intensity solar radiation, and low actual CO_2 flux in the desert are the causes of the obvious difference between the high-frequency CO_2 flux observed by IRGASON and the CO_2 flux observed by EC155 ($F_{C\text{-}op}$-$F_{C\text{-}cp}$). Through correlation analysis of $F_{C\text{-}op}$-$F_{C\text{-}cp}$ and different environmental conditions, it was found that $F_{C\text{-}op}$-$F_{C\text{-}cp}$ was highly correlated with H and each component of solar radiation (Table 2). H and DR were selected for regression analysis with $F_{C\text{-}op}$-$F_{C\text{-}cp}$ (Fig. 7), and it was found that $F_{C\text{-}op}$-$F_{C\text{-}cp}$ had a negative linear correlation

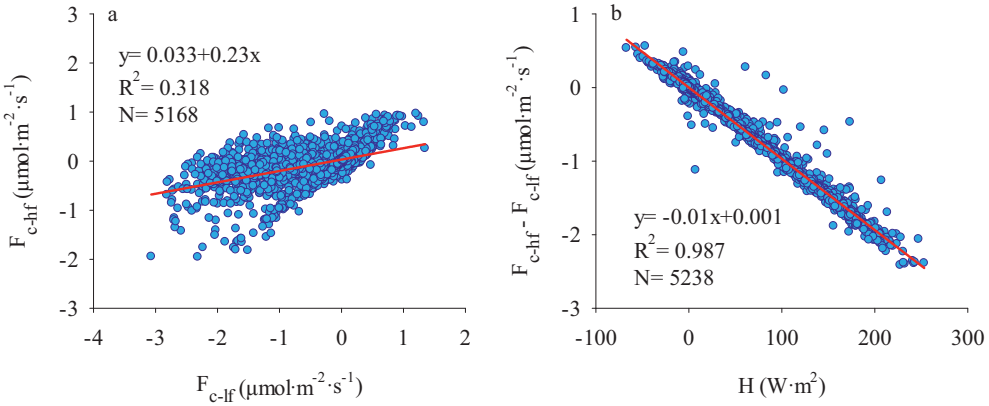

Fig. 5. In the hinterland of Taklimakan Desert, the comparison between low- and high-frequency CO_2 fluxes ($F_{C\text{-}lf}$ and $F_{C\text{-}hf}$) in 2021 (a) and the regression relationship between the difference between high- and low-frequency CO_2 fluxes and the corresponding sensible heat flux (H) (b).

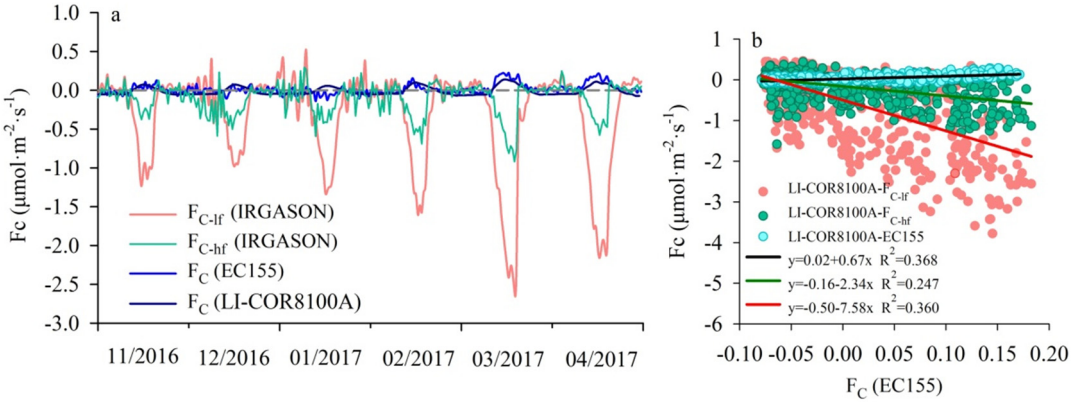

Fig. 6. Monthly average daily variation in CO_2 flux obtained by IRGASON, EC155 and LI-COR8100A (a) and their regression relationship (b) during the synchronous observation period.

Table 2
Correlation analysis results of the difference between the high-frequency CO_2 flux observed by IRGASON and the CO_2 flux observed by EC155 ($F_{C\text{-}op}$-$F_{C\text{-}cp}$) and various environmental conditions.

	H	T_a	RH	Press	DLR	DR	ULR	UR	Rn
$F_{C\text{-}op}$-$F_{C\text{-}cp}$	−0.787**	−0.312*	0.228	−0.109	−0.165	−0.809**	−0.662**	−0.808**	−0.805**

* Correlation significant at the 0.05 level.
** Correlation significant at the 0.01 level.

with both variables. This is different from the research result that the application of high-frequency CO_2 flux could essentially eliminate the difference in CO_2 flux between open- and closed-path eddy covariance in the eight northern ecosystems (Helbig et al., 2016). This further proves the particularity of desert ecosystems and shows that there is still an incomplete correction for IRGASON in desert ecosystems. This leads to abnormal CO_2 uptake signals from IRGASON in the desert. Based on this, the effect of the combined action of H and DR on $F_{C\text{-}op}$-$F_{C\text{-}cp}$ can be estimated by Eq. (1) (Fig. 8; $R^2 = 0.672$, $P < 0.01$).

$$F_{C-op} - F_{C-cp} = -0.015H - 0.004DR - 0.076 \quad R^2 = 0.675 \quad P < 0.0001 \tag{1}$$

3.5. Fluctuation of CO_2 flux in shifting sands in the hinterland of the TD

The correction relationship established above was used to correct the CO_2 flux observed by IRGASON for the study area in 2017. The corrected observation data show that the daily CO_2 exchange ($F_{C\text{-}IRGASON}$) fluctuates throughout the year in the hinterland of the TD. Most values are negative from January to March and from October to December (i.e. the shifting sand absorbs atmospheric CO_2). In contrast, most values are positive from April to September (i.e. the shifting sand releases CO_2) (Fig. 9a and 9b). In addition, there was a significant linear relationship between the daily CO_2 exchange and the daily average soil temperature difference between 0 and 10 cm ($T_{0\text{–}10\ cm}$), representing the direction and intensity of the soil heat flow (Fig. 9c; $R^2 = 0.885$, $P < 0.01$). This result is also well reflected in our previous soil respiration observation experiment in the hinterland of the TD using LI-COR8100A (Yang et al., 2020a). Gao et al. (2021) extended the conclusion to an analysis of the impact of the air–soil temperature difference on desert carbon sequestration. Thermal convection driven by the air–soil temperature difference plays a major role in absorbing and releasing CO_2 in deserts. In addition, we identified $T_{0\text{–}10\ cm}$ at 2 °C as a key threshold, which controlled the switching of the carbon source and sink of shifting sand. When $T_{0\text{–}10\ cm} > 2$ °C, the shifting sand in the desert released CO_2; when $T_{0\text{–}10\ cm} < 2$ °C, it absorbs CO_2.

In the dynamic balance of release and absorption throughout the year, absorption is relatively stronger. This suggests that the shifting sand in the hinterland of the TD shows carbon sequestration at a rate of 6.31 g m^{-2} in 2017. The absorption was the strongest in January

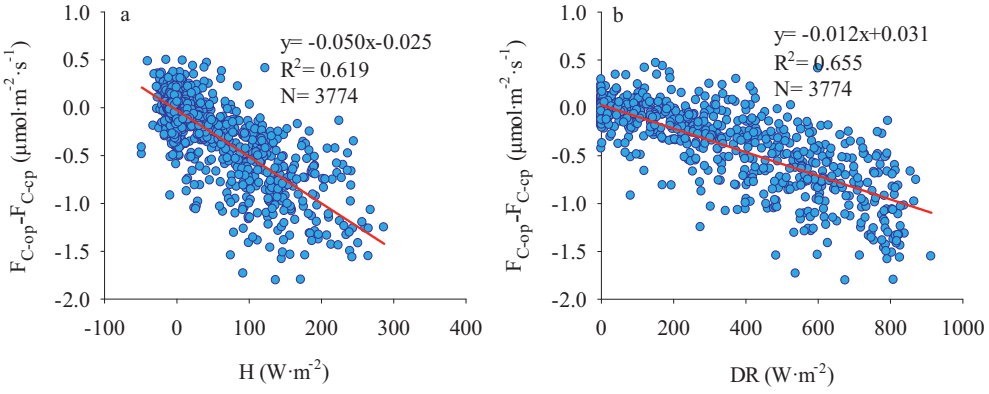

Fig. 7. Regression analysis of the difference between the high-frequency CO_2 flux observed by IRGASON and the CO_2 flux observed by EC155 ($F_{C\text{-}op}$-$F_{C\text{-}cp}$) with the sensible heat flux (H) and total solar radiation (DR). a, Regression analysis between $F_{C\text{-}op}$-$F_{C\text{-}cp}$ and H. b, Regression analysis between $F_{C\text{-}op}$-$F_{C\text{-}cp}$ and DR.

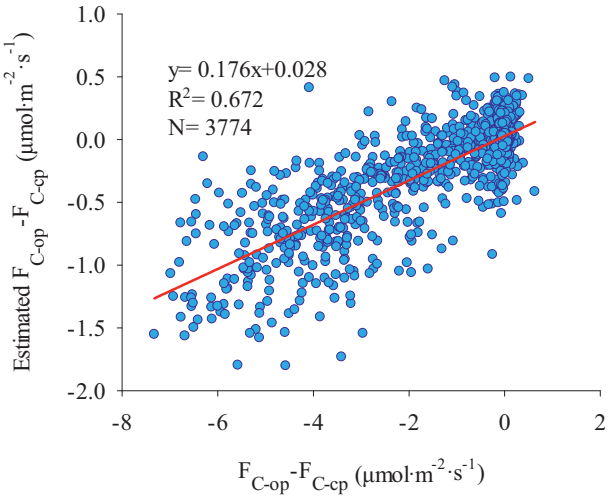

Fig. 8. Regression analysis between the difference between the high-frequency CO_2 flux observed by IRGASON and the CO_2 flux observed by EC155 ($F_{C\text{-}op}$-$F_{C\text{-}cp}$) and their estimates.

(1.84 g m^{-2} $month^{-1}$), and release was the strongest in July (up to 0.68 g m^{-2} $month^{-1}$). This result is far lower than that of other deserts (Schlesinger, 2017; Jasoni et al., 2005; Wohlfahrt et al., 2008; Liu et al., 2012; Jia et al., 2014). This result is close to our previous research result (7.11 g m^{-2} a^{-1}) and consistent with the carbon sequestration level of desert ecosystems with low productivity (Yang et al., 2020a). If the carbon sequestration rate of shifting sand in the hinterland of the TD is taken as the average state and expanded according to the area of shifting sand area in the TD (70%), the shifting sand of the TD can sequester approximately 148.85 × 10^4 tons of atmospheric CO_2 every year. This indicates that deserts also play an active role in locating missing carbon sinks and mitigating climate warming.

4. Conclusions

Through a comparative observation experiment, the CO_2 flux of shifting sand in the hinterland of the TD was measured using three instruments, and the results indicated that the abnormal negative CO_2 flux observed by IRGASON during the day would overestimate the carbon sequestration capacity of the TD. The high-frequency CO_2 flux obtained by IRGASON had a certain correction effect on the unreasonable negative CO_2 flux in the daytime compared with the low-frequency CO_2 flux. Neverheless, the correction effect was very limited in the desert ecosystem. Therefore, the CO_2 flux observed by IRGASON in desert ecosystems must be corrected further. The CO_2 flux observed by EC155 is highly consistent with that of LI-COR8100A and can reflect the real CO_2 exchange in the desert. The CO_2 flux observed by the EC155 was used to correct the IRGASON observation results. The results show that the expansion/contraction of soil air containing CO_2 caused by the change in the soil temperature difference ($T_{0–10cm}$) drives the CO_2 exchange in shifting sand. This results in the shifting sand releasing CO_2 during the day and reaching a peak at noon. At night, the shifting sand can absorb CO_2 and show carbon sequestration. Simultaneously, the daily CO_2 exchange of shifting sand follows a unimodal distribution throughout the year. From January to March and October to December, when the daily average $T_{0–10\ cm}$ is less than 2 °C, the shifting sand can absorb atmospheric CO_2. From April to September, when the daily average $T_{0–10cm}$ is greater than 2 °C, the shifting sand releases CO_2 into the atmosphere. In the dynamic

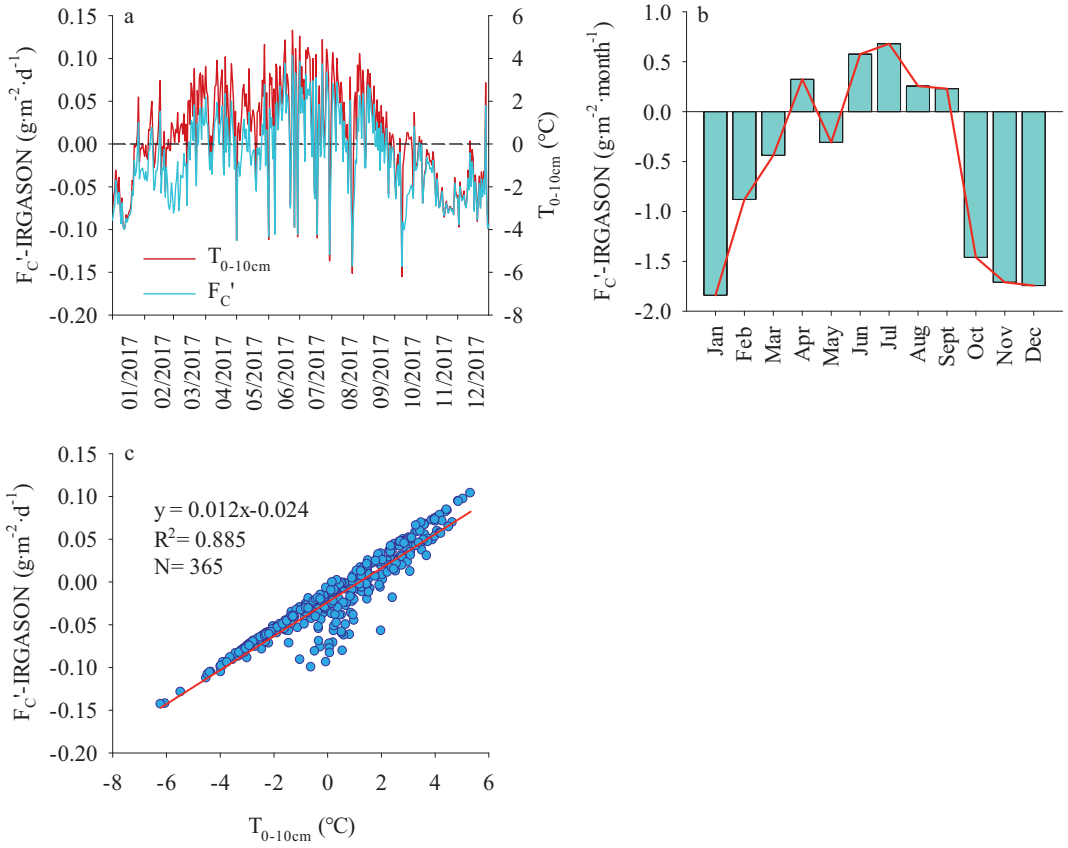

Fig. 9. High-frequency CO_2 flux values obtained by IRGASON were corrected using Eq. (1). a, Time series of the corrected daily CO_2 exchange ($F_{C\text{-}IRGASON}^{'}$) and the daily average soil temperature difference between 0 cm and 10 cm ($T_{0–10\ cm}$) in the hinterland of the TD in 2017. b, Total monthly carbon sequestration of shifting sand in the hinterland of the TD. c, Regression relationship between $F_{C\text{-}IRGASON}^{'}$ and $T_{0–10\ cm}$.

balance of release and absorption throughout the year, the absorption effect is relatively strong, indicating that the shifting sand in the hinterland of the TD shows clear carbon sequestration. The average carbon sequestration rate of shifting sand in the hinterland of the TD was 6.31 g m^{-2} a^{-1}. Suppose this carbon sequestration rate is taken as the average state and expanded according to the shifting sand area of the TD. In that case, it can sequester approximately 148.85 × 10^4 tons of atmospheric CO_2 every year. Although the carbon sequestration capacity of shifting sand in the TD is relatively weaker than that of high-productivity ecosystems such as forests and grasslands, deserts play an active role in reducing carbon emissions, mitigating climate change, and promoting sustainable social development in arid areas with deserts as the main ecosystem. Therefore, an accurate assessment of the carbon sequestration capacity of desert ecosystems is of great significance to further understand the status of deserts in the global carbon cycle and locate missing carbon sinks.

CRediT authorship contribution statement

Fan Yang: Conceptualization, Methodology, Writing-original draft, Writing-review & editing, Project administration. **Jianping Huang:** Conceptualization, Writing-original draft, Writing-review & editing, Project administration. **Xinqian Zheng:** Formal analysis. **Wen Huo:** Formal analysis. **Chenglong Zhou**: Data curation, Writing-original draft, Writing-review & editing. **Yu Wang:** Formal analysis. **Dongliang Han:** Formal analysis. **Jiacheng Gao:** Data curation. **Ali Mamtimin:** Formal analysis. **Xinghua Yang:** Writing-review & editing. **Yingwei Sun:** Data curation.

Declaration of competing interest

The authors declare that they have no known competing financial interests or personal relationships that could have appeared to influence the work reported in this paper.

Acknowledgements

This work was jointly supported by the National Natural Science Foundation of China [No. 41975010, 41991231 and 41875023], the Innovation and development project of China Meteorological Administration [CXFZ2022J043], and the Flexible Talents Introducing Project of Xinjiang [2018].

References

Baldocchi, D., 2008. 'Breathing' of the terrestrial biosphere: lessons learned from a global network of carbon dioxide flux measurement systems. Aust. J. Bot. 56, 1–26.

Baldocchi, D., 2014. Measuring fluxes of trace gases and energy between ecosystems and the atmosphere–the state and future of the eddy covariance method. Glob. Chang. Biol. 20, 3600–3609.

Bogoev, I., 2014. Improved eddy flux measurements by open-path gas analyzer and sonic anemometer co-location. 2014 EGUGA. 16 199B.

Burba, G., Mcdermitt, D., Grelle, A., Anderson, D., Xu, L., 2008. Addressing the influence of instrument surface heat exchange on the measurements of CO2 flux from open-path gas analyzers. Glob. Chang. Biol. 14, 1854–1876.

Campbell Scientific, 2017. Improved Flux Measurements from Campbell Scientific Open-Path Gas Analyzers.

Detto, M., Verfaillie, J., Anderson, F., Xu, L., Baldocchi, D., 2011. Comparing laser-based open- and closed-path gas analyzers to measure methane fluxes using the eddy covariance method. Agric. For. Meteorol. 151, 1312–1324.

El-Madany, T., Griessbaum, F., Fratini, G., Juang, J., Chang, S., Klemm, O., 2013. Comparison of sonic anemometer performance under foggy conditions. Agric. For. Meteorol. 173, 63–73.

Fa, K., Liu, J., Zhang, Y., Wu, B., Qin, S., Feng, W., Lai, Z., 2014. CO2 absorption of sandy soil induced by rainfall pulses in a desert ecosystem. Hydrol. Process. 29, 2043–2051.

Fa, K., Zhang, Y., Wu, B., Qin, S., Liu, Z., She, W., 2016. Patterns and possible mechanisms of soil CO2 uptake in sandy soil. Sci. Total Environ. 544, 587–594.

Gao, Y., Zhao, Z., Zhang, Y., Liu, J., 2021. Response of abiotic soil CO2 flux to the difference in air-soil temperature in a desert. Sci. Total Environ. 785, 147377.

Ham, J., Heilman, J., 2003. Experimental test of density and energy-balance corrections on carbon dioxide flux as measured using open-path eddy covariance. Agron. J. 95, 1393–1403.

Haslwanter, A., Hammerle, A., Wohlfahrt, G., 2009. Open-path vs. Closed-path eddy covariance measurements of the net ecosystem carbon dioxide and water vapour exchange: a long-term perspective. Agric. For. Meteorol. 149, 291–302.

Helbig, M., Wischnewski, K., Gosselin, G., Biraud, S., Bogoev, I., Chan, W., Euskirchend, E., Glenn, A., Marsh, P., Quinton, W., Sonnentag, O., 2016. Addressing a systematic bias in carbon dioxide flux measurements with the EC150 and the IRGASON open-path gas analyzers. Agric. For. Meteorol. 228–229, 349–359.

Jasoni, R., Smith, S., Arnone, J., 2005. Net ecosystem CO2 exchange in Mojave Desert shrublands during the eighth year of exposure to elevated CO2. Glob. Chang. Biol. 11, 749–756.

Jia, X., Zha, T., Wu, B., Zhang, Y., Gong, J., 2014. Biophysical controls on net ecosystem CO2 exchange over a semiarid shrubland in Northwest China. Biogeosciences 11, 4679–4693.

Liu, R., Li, Y., Wang, Q., 2012. Variations in water and CO2 fluxes over a saline desert in western China. Hydrol. Process. 26, 513–522.

Ma, J., Wang, Z., Stevenson, B., Zheng, X., Li, Y., 2013. An inorganic CO2 diffusion and dissolution process explains negative CO2 fluxes in saline/alkaline soils. Sci. Rep. 3, 20–25.

Ma, J., Liu, R., Tang, L., Lan, Z., Li, Y., 2014. A downward CO2 flux seems to have nowhere to go. Biogeosciences 11, 6251–6262.

Moore, C., 1986. Frequency response corrections for eddy correlation systems. Bound.-Layer Meteorol. 37, 17–35.

Novick, K., Walker, J., Chan, W., Schmidt, A., Sobek, C., Vose, J., 2013. Eddy covariance measurements with a new fast-response, enclosed-path analyzer: spectral characteristics and cross-system comparisons. Agric. For. Meteorol. 181, 17–32.

Ono, K., Miyata, A., Yamada, T., 2008. Apparent downward CO2 flux observed with open-path eddy covariance over a non-vegetated surface. Theor. Appl. Climatol. 92, 195–208.

Rannik, U., Vesala, T., 1999. Autoregressive filtering versus linear detrending in estimation of fluxes by the eddy covariance method. Bound.-Layer Meteorol. 91, 259–280.

Russell, E., Dziekan, V., Chi, J., Waldo, S., Pressley, S., O'Keeffe, P., Lamb, B., 2019. Adjustment of CO2 flux measurements due to the bias in the EC150 infrared gas analyzer. Agric. For. Meteorol. 276, 107593.

Schlesinger, W., 2017. An evaluation of abiotic carbon sinks in deserts. Glob. Chang. Biol. 23, 25–27.

Schotanus, P., Nieuwstadt, F.T.M., Debruin, H.A.R., 1983. Temperature measurement with a sonic anemometer and its application to heat and moisture fluxes. Bound.-Layer Meteorol. 26, 81–93.

Song, X., Yu, G.R., Liu, Y.F., Sun, X.M., Ren, C.Y., Wen, X.F., 2005. Comparison of flux measurement by open-path and close-path eddy covariance systems. Sci. China Ser. D Earth Sci. 48, 74–84.

Stone, R., 2008. Have desert researchers discovered a hidden loop in the carbon cycle? Science 320, 1409–1410.

Vickers, D., Mahrt, L., 1997. Quality control and flux sampling problems for tower and aircraft data. J. Atmos. Ocean. Technol. 14, 512–526.

Wang, L., Lee, X., Wang, W., Wang, X., Wei, Z., Fu, C., Gao, Y., Lu, L., Song, W., Su, P., Lin, G., 2017. A meta-analysis of open-path eddy covariance observations of apparent CO2 flux in cold conditions in FLUXNET. J. Atmos. Ocean. Technol. 34, 2475–2487.

Wang, W., Xu, J., Gao, Y., Bogoev, I., Cui, J., Deng, L., Hu, C., Liu, C., Liu, S., Shen, J., Sun, X., Xiao, W., Yuan, G., Lee, X., 2016. Performance evaluation of an integrated open-path eddy covariance system in a cold desert environment. J. Atmos. Ocean. Technol. 33, 2385–2399.

Wang, Y., Wang, J., Yan, C., 2005. <year>2005</year>. Data Set of Desert (Sand) Distribution in China With Scale of 1:100000. Cold and Arid Regions Science Data Center at Lanzhou.

Webb, E.K., Pearman, G.I., Leuning, R., 1980. Correction of flux measurements for density effects due to heat and water-vapour transfer. Q. J. R. Meteorol. Soc. 106, 85–100.

Wilczak, J.M., Oncley, S.P., Stage, S.A., 2001. Sonic anemometer tilt correction algorithms. Bound.-Layer Meteorol. 99, 127–150.

Wohlfahrt, G., Fenstermaker, L., Arnone III, J., 2008. Large annual net ecosystem CO2 uptake of a Mojave Desert ecosystem. Glob. Chang. Biol. 14, 1475–1487.

Yang, F., Ali, M., Zheng, X., He, Q., Yang, X., Huo, W., Liang, F., Wang, S., 2017. Diurnal dynamics of soil respiration and the influencing factors for three land-cover types in the hinterland of the Taklimakan Desert, China. J. Arid Land 9, 568–579.

Yang, F., Huang, J., He, Q., Zheng, X., Zhou, C., Pan, H., Huo, W., Yu, H., Liu, X., Meng, L., Han, D., Ali, M., Yang, X., 2020a. Impact of differences in soil temperature on the desert carbon sink. Geoderma 379, 114636.

Yang, F., Huang, J., Zhou, C., Yang, X., Ali, M., Li, C., Pan, H., Huo, W., Yu, H., Liu, X., Zheng, X., Han, D., He, Q., Meng, L., Chang, J., 2020b. Taklimakan desert carbon sink decreases under climate change. Sci. Bull. 65, 431–433.

Yang, F., He, Q., Huang, J., Ali, M., Yang, X., Huo, W., Zhou, C., Liu, X., Wei, W., Cui, C., Wang, M., Li, H., Yang, L., Zhang, H., Liu, Y., Zheng, X., Pan, H., Jin, L., Zou, H., Zhou, L., Liu, Y., Zhang, J., Meng, L., Wang, Y., Qin, X., Yao, Y., Liu, H., Xue, F., Zheng, W., 2021. Desert environment and climate observation network over the Taklimakan Desert. Bull. Am. Meteorol. Soc. 102 E1172-E1191.

Yu, G., Sun, X., 2017. Principles of Flux Measurement in Terrestrial Ecosystems. Higher Education Press 243 pp.